

Quantum and classical algorithms for daily railway rolling stock circulation plans

Ewa Kędziera*, Wojciech Gamon†, Mátyás Koniorczyk‡, Zakaria Mzaouali§,
Andrea Galadíkova¶, Krzysztof Domino||

December 23, 2025

Abstract

We study daily rolling stock circulation planning for electric multiple units (EMUs) on a regional passenger network, focusing on services where identical EMUs may be coupled in pairs on selected routes. Motivated by the operational needs of the regional operator Silesian Railways in Poland, we formulate an acyclic mixed-integer linear program on a one-day horizon that incorporates depot balance constraints, demand-driven seat and bicycle capacity limits (which is a new aspect requested by the regional operator and local society of passengers), and simple crew availability constraints. The model is designed to support both baseline planning and disruption management under increased passenger demand. Using a graph-hypergraph representation of trips and single or coupled EMU movements, we first solve the problem with a classical ILP solver. We then derive a Quadratic Unconstrained Binary Optimization (QUBO) reformulation - which is frequently used as the input for quantum optimization - and evaluate its solution by quantum annealing on D-Wave Advantage systems and by the classical quantum-inspired VeloxQ solver. Computational experiments on real-world instances from the Silesian network, with up to 404 train trips and 11 EMU types, show that the ILP approach can obtain high-quality daily circulation plans within at most about 40 minutes,

*ekedziera@iitis.pl, Institute of Theoretical and Applied Informatics, Polish Academy of Sciences, Gliwice

†ORCID: 0000-0002-6015-2597, Silesian University of Technology, Department of Railway Transport, Faculty of Transport and Aviation Engineering, Gliwice, Poland

‡ORCID: 0000-0002-2710-493X, HUN-REN Wigner Research Centre for Physics, Department of Quantum Optics and Quantum Information, Budapest, Hungary

§ORCID: 0000-0003-3948-1318, Eberhard Karls Universität Tübingen, Institut für Theoretische Physik, Tübingen, Germany; Forschungszentrum Jülich, Jülich Supercomputing Center, Jülich, Germany

¶University of Žilina, Department of Mathematical Methods and Operations Research, Faculty of Management Science and Informatics, Žilina, Slovakia

||kdomino@iitis.pl, ORCID: 0000-0001-7386-5441, Institute of Theoretical and Applied Informatics, Polish Academy of Sciences Bałtycka 5, 44-100 Gliwice

whereas current quantum and quantum-inspired solvers are restricted to substantially smaller sub-instances (up to 51 and 78 train trips, respectively) due to embedding and QUBO size limitations. These results quantify the present frontier of QUBO-based methods for rolling stock circulation and point towards hybrid decision-support architectures in which quantum or quantum-inspired optimizers address only local subproblems within a broader classical planning framework.

Keyword

Rolling stock circulation planning; stakeholder-driven approach; passenger and bicycle capacity; quantum annealing; VeloxQ QUBO solver

1 Introduction

Optimization of processes in railway transport is essential to ensure its efficient operation. The best way to develop such models is to work closely with stakeholders. Therefore, the research problem addressed in this work is based on the specific requirements of the local community of passengers as well as the regional passenger rail operator — Silesian Railways (pl. Koleje Śląskie).

Our goal is to develop a flexible model, yielding a reactive rolling stock plan on an operational time horizon, subject to crew availability constraints, that can respond efficiently to unexpected events. Our model supports different optimization objectives, aiming to balance two primary goals: maximizing the rolling stock reserve and minimizing the operational costs associated with rolling stock usage. Due to the requirements of the local society of passengers and the railway operator, we introduce the bicycle capacity constraint, as the operator serves many tourist destinations.

Rolling stock circulation models are essentially modifications of set-flow models, which do not scale well to large problem instances. In direct implementations of quantum and quantum-inspired approaches, the optimization problem (a variant of the set-flow problem) is formulated as a Quadratic Unconstrained Binary Optimization (QUBO) problem, which also incurs significant overhead for large instances. Recall that the QUBO formulation is the most recognisable input for quantum (quantum-inspired) optimisation; however, we recognise that there are also other approaches, for example, variational quantum algorithms with qubit-efficient encodings [1]. Based on these observations, we assess the current frontier of QUBO-based quantum and quantum-inspired approaches in comparison with classical approaches. Figure (1) describes the workflow of our work.

Classical vs. Quantum Approaches for EMU Circulation

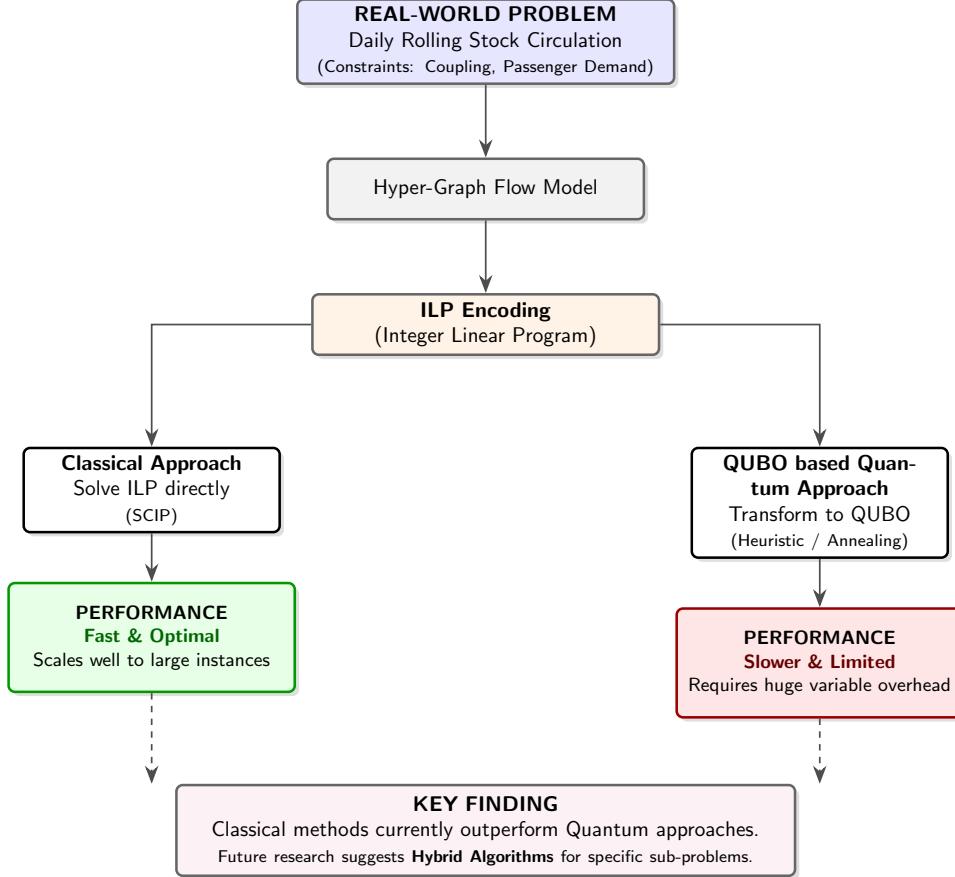


Figure 1: The workflow of the paper

1.1 Problem Description

We start the problem description from the practical point of view. The railway operator's staff, equipped with knowledge of the timetable, the available railway vehicles and their technical and operational parameters, the pool of drivers based in depots, and expected passenger demand, prepare detailed planning tables. These tables assign individual EMU (or pairs of EMUs in some predefined cases) to specific trains (operating on designated routes at specified times) while adhering to all internal and external constraints. Additionally, given the baseline plan, the operator must respond to disruptions, such as increased passenger demand, rolling stock breakdowns, and other issues, in order to minimize the propagation of disturbances throughout the network. We focus on the acyclic rolling stock planning on the operational time horizon with the drivers' ability aspect, yielding either the original vehicle circulation plan or its version given some disturbances (i.e. increased

passenger or bicycle demand). Hereby, we recognise that we do not create an entire driver roster (including driving times, breaks, and many other aspects) but only introduce some constraints to check the drivers' ability.

A crucial aspect of rolling stock circulation planning is the need for coordination with infrastructure management. The operator values having multiple solutions to the problem, each with different objective values, available within the decision support system (DSS). This allows the dispatcher to make the final decision while maintaining communication with the infrastructure manager.

1.2 Literature review

The optimization of the rolling stock circulation has been extensively studied in many detailed models using both exact and heuristic methods. Due to the strong interdependence between timetable structure, fleet availability, and operational constraints, a wide spectrum of mathematical programming approaches has emerged. Rolling stock circulation is most commonly formulated as a constrained network-flow problem [2], either in arc-based or path-based form, and often solved through advanced decomposition or column generation techniques. More recent approaches incorporate additional operational realism, including capacity constraints, stochasticity, or multi-stage decision structures, see e.g. [3].

When passenger demand is taken into account, a major challenge in rolling stock circulation planning becomes the use of flexible train compositions, which allow vehicle capacities to match peak-hour flows while respecting operational constraints. In Central European operational practice, frequent modifications of EMU compositions are less common, particularly in winter conditions. Therefore, our model allows for joining and splitting EMUs, but rather occasionally (for predefined trains), reflecting realistic operational policies.

To illustrate the sizes of the problems that are accessible on the available hardware, we refer to the following literature. A classical model that is conceptually closest to our formulation is the work of Fioole et al. [4], who proposed one of the first mixed-integer models capable of handling rolling stock circulation together with operationally realistic combining and splitting of EMUs. Their formulation explicitly models train compositions and allows changes in the number of units assigned to each trip, enabling the representation of coupling/uncoupling operations subject to station-specific constraints. A trip is defined as a sequence of train movements during which the composition cannot change, which corresponds to the structure used in our model.

An important contribution of their work is the introduction of seat-shortage kilometers as a service-quality metric. It measures, for each trip, the expected number of passengers without seats multiplied by the trip distance

and summed over all services. This idea is closely related to the demand-driven capacity modelling used in our classical ILP formulation.

For validation, the authors used a real-world dataset from the Dutch operator NS Reizigers, consisting of 665 trips executed by roughly 50 three-car and 35 four-car EMUs. Only limited composition changes were allowed, and all splitting events were predefined by the timetable. The resulting MIP contained over 50,000 variables and 30,000 constraints, and was solvable using CPLEX within 2-4 hours, depending on the objective configuration.

Flexible train composition is also explored in [5]. Authors propose a MILP model that simultaneously optimizes the train timetable and the rolling stock circulation plan, allowing composition changes at terminal stations. A similar mixed-integer linear programming formulation is presented in [6], where vehicle assignment and capacity constraints are explicitly integrated into the timetable optimization process, representing one of the early formulations of joint timetable–circulation optimization. However, the authors report that the optimal solution could not be obtained within 24 hours of computation, reflecting the high computational complexity of their formulation. The consideration of passenger demand in the design of the branch-and-price algorithm was also addressed by [7]. In their conception, demand affects the minimum required capacity of each train service, and therefore influences which rolling stock types or compositions may appear in the generated columns.

More sophisticated multi-stage models incorporating passenger demand have also been proposed, although they tend to be operator-specific and less suitable as general benchmarking instances.

Wang et al. [8] introduce an iterative nonlinear programming (INP) method that alternates between a nonlinear capacity-allocation subproblem and a circulation subproblem based on MILP. The two stages are solved sequentially, using the solution of one to update and refine the other until convergence to a feasible solution of the original MINLP. Applied to 122 train services, their MILP subproblem required approximately 5 hours and approached optimality. Pan et al. [3] address flexible train composition planning under stochastic passenger demand and solve the resulting MILP using a Benders decomposition approach. Their computational experiments on an instance with 38 train services required approximately 7 hours of computation.

The study in [9] highlights the importance of jointly modelling periodic and aperiodic timetabling together with rolling stock circulation. To address the high dimensionality of the resulting formulation, authors propose a three-dimensional space–time–state network and solve it using a Lagrangian relaxation decomposition. A closely related three-dimensional network structure is adopted by Niu et al. [10], who apply an ADMM-based decomposition mechanism to coordinate the resulting subproblems. Finally, Shen et al. [11] propose a hybrid meta-heuristic combining a self-adjusting genetic algorithm

(SGA), large-neighborhood search (LNS), and a Pareto separation operator (PSO), demonstrating that this type of hybrids can effectively handle the computational complexity of integrated timetabling and vehicle scheduling.

To assess the size of instances that can be handled with more advanced exact approaches, Nishi et al. [12] apply column generation with Lagrangian relaxation to solve an instance with 300 trips, where the binary decision variables determine whether a transition between two trips is assigned within a specific rotation cycle. Their linear objective minimizes the number of maintenance arcs and transitions between operational days, reflecting the goal of generating operationally efficient rotation plans. Pan et al. [13] extend this idea to flexible train compositions using a column-generation-based diving heuristic capable of jointly generating both the timetable and the circulation. Complementary to these approaches, Bao et al. [14] demonstrate that simulated annealing can also be applied to flexible-composition problems as a heuristic alternative.

Exact methods can also handle large-scale rolling stock planning problems. Gao et al. [15] develop a branch-and-price algorithm based on an event-node rotation network for weekly planning in high-speed rail. In their formulation, nodes represent operational events such as trip starts and ends, maintenance activities, or idle periods, while arcs encode possible transitions between these events, capturing the flow of train units through different operational states. The resulting graph is then encoded as an ILP, where binary decision variables select the arcs that form feasible weekly rotations. An important contribution in a similar direction is the hypergraph-based formulation of Borndörfer et al. [16], where train rotations are modelled jointly with feasible multi-unit compositions under platform-length, orientation, and maintenance restrictions. Hyperarcs represent admissible compositions of multiple train units, and the optimization is solved by a hierarchical column-generation scheme that progresses from coarse to fine levels of detail.

Two-stage exact approaches have also been explored in the literature. Haahr et al. [17] address long-term rolling stock planning and short-term rescheduling under disturbances using MILP and column generation. Their approach minimizes costs related to trip cancellations, seat shortages, and turnaround operations, and can handle large-scale instances, although it does not incorporate flexible train compositions or demand-driven capacity constraints. Related work such as [18] focuses on alternative objectives — e.g., stabilizing train headways while minimizing fleet size — further illustrating the diversity of modelling goals in rolling stock optimization.

In summary, the literature on rolling stock circulation offers a wide range of modelling paradigms, including network-flow formulations, mixed-integer models with flexible train compositions, decomposition-based approaches, and large-scale exact and metaheuristic methods. While many studies address capacity constraints, passenger demand, or operational feasibility, only a limited subset simultaneously considers flexible EMU compositions to-

gether with demand-driven capacity requirements in a way that remains computationally tractable for real-world instances. (There is also scarce literature on constraints tied to bicycle capacity.) Moreover, existing works differ substantially in modelling detail, scope, and solution methodology, making it difficult to directly compare contemporary approaches or to assess their frontier for large-scale practical applications. These observations naturally lead to several research gaps, which we discuss in the following section.

1.3 Research gaps

We recognize the following research gaps. Existing optimization models can grow to sizes that are difficult to handle for realistic instances. In theory, quantum computing promises to address such large-scale problems in a reasonable time once the technology matures. However, we are currently in the NISQ era, in which quantum devices are small and prone to errors. It is therefore important to assess the present stage of development of quantum approaches for the practical problem of railway rolling stock circulation planning. There is little literature on quantum computing or quantum-inspired approaches for the rolling stock circulation planning, to our knowledge, limited to the article [19], where the problem of rolling stock circulation planning on the German Railways network was examined.

As quantum devices are small and prone to error, a hybrid quantum-classical approach [20] has been applied therein and to a somewhat similar railway rescheduling problem [21]. However, such hybrid solvers are proprietary, and it is difficult to assess the potential impact of the quantum or quantum-inspired part of the algorithm on the overall optimization performance.

Concluding, although quantum computing promises to solve large NP-hard problems, there is a lack of research on the actual frontier between classical, quantum-inspired and quantum approaches for railway rolling stock planning. To fill these research gaps, we investigate this frontier (in the context of QUBO formulation) for a practical railway rolling stock planning problem. Our contributions are:

- practical ILP/hyper-graph model with EMU coupling for pre-selected destinations and demand-driven capacity,
- QUBO mapping and scaling analysis specific to rolling stock,
- empirical comparison ILP vs D-Wave vs VeloxQ [22, 23, 24, 25, 26] on real data, and
- implications for future hybrid architectures.

To be complete, as stakeholder-driven research, we enrich the model with the bicycles’ capacity requirements, as the regional operator, beyond commuters, also serves an increasing number of tourists. To place our paper in the literature precisely, please refer to Tab. 1

Table 1: Comparison of representative rolling stock circulation models (key features). **Legend:** H = planning horizon (Day = daily, Week = weekly); C = EMU coupling/splitting; D = demand-driven capacity constraints; M = stochastic or multi-stage structure; \checkmark = fully modeled, \checkmark^* = modeled with predefined or restricted coupling locations, \circ = limited or scenario-based, $-$ = not considered; ILP = integer linear programming, MILP = mixed integer linear programming, INP = iterative nonlinear programming, BD = Benders decomposition, CG = column generation, HG = hypergraph.

Reference	H	C	D	M	Method
Fioole et al. [4]	Day	\checkmark	\checkmark	$-$	ILP
Espinosa et al. [6]	Day	$-$	\checkmark	$-$	MILP
Wang et al. [8]	Day	\circ	\checkmark	\checkmark	INP/MILP
Pan et al. [3]	Day	\checkmark	\checkmark	\checkmark	MILP+BD
Borndörfer et al. [16]	Week	\checkmark	$-$	$-$	HG+CG
Grozea et al. [19]	Day	$-$	$-$	$-$	QUBO
This work	Day	\checkmark^*	\checkmark	\circ	HG+ILP/QUBO

2 Model

In this section, we present a mathematical model for the railway problem under study, namely EMU circulation planning on the operational time horizon, using an acyclic setting. Technically, we encode the problem using a graph-based approach inspired by the *Graph Flow* method discussed in chapter 10 of [2]. In our model, we use the graph / hyper-graph approach, modelling trips as nodes, EMU transfer between trips as arcs, and transfers of coupled EMUs as hyper-arcs.

By a trip, we mean a train journey from its origin station to its destination station; hence, we use the terms train and trip interchangeably throughout the paper. Our problem is defined by a timetable T , composed of train trips $\tau \in T$. Each trip has a departure time $t_{\text{start}}(\tau)$ and arrival time $t_{\text{end}}(\tau)$. For each trip, we consider in the model only the departure from the first station and the arrival at the last station - we do not consider all stops during the trip - such an approach limits the model’s size and increases the size of tractable problems.

To cover the timetable, we consider EMU types $r \in R$ and depots $d \in D$, where $N(v_d)_r$ denotes the number of EMUs of type r in depot d , and there

are distinct $|R|$ such parameters for each depot. According to the specifics of our industrial partner, we support EMU couplings under the following limitations. We consider only couplings of EMUs of the same type (denoted by r), in pairs of at most two EMUs, and only for a selected subset of trips $\tau'' \in T'' \subset T$ predefined based on the partner's requirements. This assumption simplifies the model while retaining practical relevance.

Let $\tau' \in T'$ be trips that can be served only by the single EMU, and $\tau'' \in T''$ trips that can be served by either single or multiple EMUs, then $T = T' \cup T''$ and $T' \cap T'' = \emptyset$.

The problem is mapped to a (hyper-)graph composed of:

1. nodes $v \in V$ representing particular trips (including also service trips, if necessary). For each node, we store train-specific data, namely passenger (and bicycles) demand, allowed rolling stock compositions, whether the trip is obligatory, and the trip length (for cost calculations);
2. arcs $h_{v,v',r}$ (or hyper-arcs for coupled EMUs) depicting the use of an EMU of type r on trip v followed by trip v' . To (hyper-)arcs we assign fixed and variable costs, as well as the seating and bicycle capacities of trips they point to.

As represented in Fig. 2, hyper-arcs for coupled EMUs have one of the following forms:

1. $(h_{(v_1,v_2),(v',v'),r})$ representing the coupling of two EMUs arriving on trains v_1 and v_2 to form a multiple-unit composition for v' (the hyper-arc is partially directed in the sense $[v_1, v_2] \rightarrow [v']$);
2. $(h_{(v,v),(v',v'),r})$ representing coupled EMUs transferring from train v to train v' , (the order is $[v] \rightarrow [v']$)
3. $(h_{(v,v),(v'_1,v'_2),r})$ representing a coupled pair of EMUs on trip v that is decoupled into two single-EMU services on trips v'_1, v'_2 , (the hyper-arc is partially directed in the sense $[v] \rightarrow [v'_1, v'_2]$)

Technically, arcs have to fulfill the following conditions to be considered as the solution:

1. for each line, there is a subset of EMU types that are allowed to serve it;
2. there is the subset of EMU types that can be coupled in pairs, only on the pre-selected trips - T'' ;
3. arcs and hyper-arcs have temporal feasibility constraints. The transfer time between trains is bounded from below by $\delta(h_{v,v',r})$ and from above by $\Delta(h_{v,v',r})$; the latter bound limits model complexity and, to some extent, accounts for station capacity. When these bounds are constant across the instance, we simply use δ and Δ ;

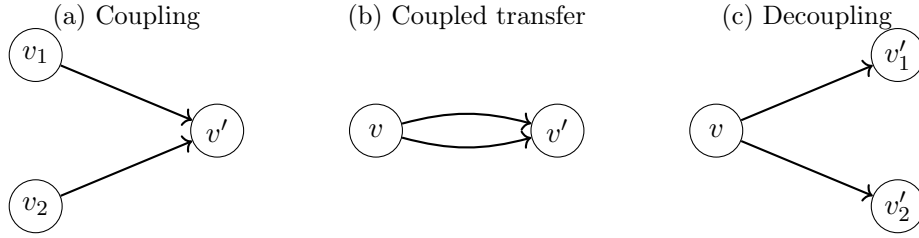


Figure 2: Illustration of the three hyper-arc types: (a) coupling of two EMUs into a multiple-unit service, (b) transfer of a coupled composition represented by a hyper-arc composed of two parallel arcs, and (c) decoupling into two single-EMU services.

4. an arc may originate in a depot if EMUs of the corresponding type are available at that depot.

2.1 ILP encoding

The objective is to minimize the number of EMUs in operation to build a reserve and to reduce operating costs weighted by parameter. The daily schedule must cover all trips, maintain continuity of rolling-stock circulation, and satisfy bounds on the number of units of each type that start and end the day at a given location. Rolling-stock capacity must meet passenger and bicycle demand, and operations must respect limits on the number of drivers available at any given time.

For mathematical purposes, we introduce the following mathematical definitions.

1. Sets
 - (a) Let T denote the timetable, and let $\tau \in T$ be an individual trip.
 - (b) Let H be the set of all possible arcs and hyper-arcs that are solution candidates (given technical requirements). The set H is supposed to cover all trains under the conditions described above and may also include optional service trains linking depots with the starting or ending points of trains.
 - (c) Let $H(\tau) \subset H$ be the set of all available arcs or hyper-arcs that can cover (i.e. point to) trip τ .
 - (d) Let R be the set of EMUs types, and let $r \in R$.
 - (e) Let $H(v)_r^{\text{in}}, H(v)_r^{\text{out}}$ be the sets of incoming and outgoing arcs (and hyper-arcs), respectively, incident to node v and corresponding to EMU type r .
 - (f) Let D be the set of depots, and let $d \in D$. In this model, depots are both initial and final graph nodes. A service train leaving

depot d (at the beginning of the schedule) is represented by $v_d \in V_d$, while a service train entering depot d (up to the end of the schedule) is represented by $v'_d \in V'_d$.

- (g) Let $H(t, d)$ be the set of arcs that require a driver from depot d at time t (we assume a fixed, predefined depot–driver–train assignment, but generalization is straightforward).

2. Parameters

- (a) Let α be a weighting coefficient that balances the different parts of the objective function (namely the operational costs versus the number of EMUs used).
- (b) Let $k(h) \in \{1, 2\}$ be the number of EMUs in the train (or each of the trains) that the (hyper-)arc h is pointing to. For simple arcs we have $k(h) = 1$, whereas for hyper-arcs we allow $k(h) \in \{1, 2\}$. Analogously, let $k'(h)$ be the number of EMUs in the train (or each of the trains) from which the arc (or hyper-arc) originates.
- (c) Let $N(v_d)_r, n(v_d)_r$ denote the maximal and minimal number, respectively, of EMUs of type r that can be deployed from depot d .
- (d) Analogously, let $N'(v'_d)_r, n'(v'_d)_r$ denote the maximal and minimal number, respectively, of EMUs of type r that must enter depot d (up to the end of the schedule).
- (e) Let p_h and b_h be the shortage of passenger seats and bicycle places, respectively, for the trip (or trips) that (hyper-)arc h points to, and let δp_h (δb_h) be the acceptable shortage on that trip.
- (f) Let c_h be the operational cost of a particular trip (or trips), the (hyper-)arc h points to.
- (g) Let $A(t, d), a(t, d)$ be the maximal and minimal number, respectively, of drivers employed at time t , and registered at depot d (a generalization to other crew members is also possible).

3. Variables

- (a) Let $x_h \in \{0, 1\}$ be a decision variable that is equal to one if and only if $h \in H$ is part of the solution.

Then we have the (hyper-)Graph Flow problem:

$$\min_{\vec{x}} \left(\sum_{h \in H} \alpha c_h x_h + \sum_{d \in D} \sum_{v_d \in V_d} \sum_r \sum_{h \in H(v_d)_r} k'(h) x_h \right) \quad (1)$$

$$\sum_{h \in H(\tau)} x_h = 1 \quad \forall \tau \in T, \quad (2)$$

$$\sum_{h \in H(v)_r^{\text{in}}} k'(h)x_h = \sum_{h \in H(v)_r^{\text{out}}} k(h)x_h \quad \forall v \in V, \forall r \in R, \quad (3a)$$

$$\sum_{r \in R} \sum_{h \in H(v)_r^{\text{out}}} x_h \leq 1 \quad \forall v \in V, \quad (3b)$$

$$0 \leq n(v_d)_r \leq \sum_{h \in H(v_d)_r} k'(h)x_h \leq N(v_d)_r \quad \forall d \in D, \forall v_d \in V_d, \forall r, \quad (4)$$

$$0 \leq n'(v'_d)_r \leq \sum_{h \in H(v'_d)_r} k(h)x_h \leq N(v'_d)_r \quad \forall d \in D, \forall v'_d \in V'_d, \forall r, \quad (5)$$

$$\sum_{h \in H: p_h > \delta p_h} x_h = 0, \quad (6)$$

$$\sum_{h \in H: b_h > \delta b_h} x_h = 0, \quad (7)$$

$$0 \leq a(t, d) \leq \sum_{h \in H(t, d)} k(h)x_h \leq A(t, d) \quad \forall d \in D, \forall t \in \{t_1, t_2, t_3, t_4, \dots\}, \quad (8)$$

$$x_h \in \{0, 1\} \quad \forall h \in H. \quad (9)$$

Objective Eq. (1) is the linear objective with two components: the operational costs and the number of EMUs deployed. Beyond the hard capacity limits given by Eq. (4)), we explicitly penalize the number of EMUs used in order to increase the available rolling stock reserve.

As discussed later, the fleet size is considered to be predefined and constant, and is only affected by breakdowns. Although we concentrate on operational cases, to improve resilience to further disruptions, one of the objectives in our model is to maximize the rolling stock reserve so that additional unexpected events can be handled.

Constraints Eq. (2) is the coverage constraint, i.e., each train is covered once and only once. Eq. (3) enforces rolling stock continuity constraint: Eq. (3a) balances incoming and outgoing flow for each node and EMU type, while Eq. (3b) ensures that at most one arc or hyper-arc leaves the node (this is not guaranteed by Eq. (2), which only handles the incoming flow to a trip). In Eq. (4), we check whether the rolling stock constraint is met, i.e., each depot must dispatch a number of EMUs of each type within a predefined range. Analogously, Eq. (5) requires that the number of EMUs returning to each depot by the end of the schedule lies within a given range. (These can be used to enforce equal numbers in and out of each depot by setting $n(v_d)_r = N(v_d)_r$ and $n'(v'_d)_r = N'(v'_d)_r$).

Eqs. (6)–(7) impose capacity constraints: trains must provide sufficient capacity for passengers and bicycles, and the shortage of seats or bicycle places cannot exceed the allowed level. In the case of a hyper-arc h pointing to two trips, these conditions must be checked for both trips inclusively.

We also propose constraints on the required number of crew. The crew constraint in Eq. (8), will be discussed in detail below. We focus on drivers, but the generalization to other crew members is straightforward. Let $t_1, t_2, t_3, t_4 \dots$ be the time instants at which the number of drivers is evaluated; at each such time we impose a general constraint on driver availability.

A potential extension would be to consider drivers with specific authorizations for the given rolling stock types and lines. Let $A(t, d, l)$ and $a(t, d, l)$ denote the maximum and minimum number, respectively, of drivers with license $l \in L$ available at depot d and time t . Let $H(t, d, l)$ be the set of arcs that require a driver from depot d at time t and with license l . Then

$$\forall d \in D \forall t \in \{t_1, t_2, t_3, t_4, \dots\} \forall l \in L \sum_{h \in H(t, d, l)} k(h)x_h \leq A(t, d, l) \quad (10)$$

and a lower bound based on $a(t, d, l)$ can be included analogously if needed.

We assume the worst-case limit

$$|H(\tau)| \leq |T|^2 |R| \quad (11)$$

where $|R|$ is the number of types of EMUs. Here, the arc to the given train can be from all other trains, with all possible EMU types, and the square is for all combinations of joining EMUs. Regarding scaling, in the worst case the problem size (i.e., the number of binary variables $|\vec{x}|$, equal to the number of arcs and hyper-arcs) is

$$|\vec{x}| \leq |T| \cdot |T|^2 |R| \quad (12)$$

However, since the coupling of EMUs is allowed only in a predefined subset of trips $T'' \subset T$, the actual problem is smaller. In the worst case we obtain

$$|\vec{x}| \leq |T'|^2 \cdot |R| + |T''|^3 \cdot |R| \quad (13)$$

2.2 QUBO encoding

As discussed before, we have selected the QUBO-based approach as it is native to the quantum annealing, which, at the current state-of-the-art, can handle relatively large (compared with other paradigms of quantum computing) optimization problems in terms of the number of binary variables. For quantum and quantum-inspired approaches, we encode the problem as the Quadratic Unconstrained Binary Optimization (QUBO). In such implementation, we treat all constraints as soft with large penalties and then

post-filter infeasible solutions, rather than trying to guarantee feasibility by construction. We follow a standard ILP-to-QUBO transformation as in [27].

The general QUBO form is as follows

$$\min_{\vec{y}} \vec{y}^T Q \vec{y} \quad (14)$$

where \vec{y} is a vector of binary variables, $\forall_i y_i \in \{0, 1\}$. In our case, \vec{y} collects both the decision variables x_h from Section 2.1 and additional auxiliary slack variables $\forall_i s_i \in \{0, 1\}$. We transform the problem defined by Eqs. (1)–(9) into the following quadratic form:

$$\min_{\vec{y}} (f(\vec{y}) + P_1(\vec{y}) + P_2(\vec{y}) + P_3(\vec{y}) + P_4(\vec{y}) + P_5(\vec{y})) \quad (15)$$

where the objective is:

$$f(\vec{y}) = \sum_{h \in H} \alpha c_h x_h + \sum_{d \in D} \sum_{v_d \in V_d} \sum_r \sum_{h \in H(v_d)_r} k'(h) x_h. \quad (16)$$

In constraint terms P_1, \dots, P_5 we use penalty coefficients: $\lambda_1, \dots, \lambda_5$ are penalty coefficients used to convert the constrained problem into an unconstrained QUBO. The coverage constraint from Eq. (2) yields following QUBO terms

$$P_1(\vec{y}) = \lambda_1 \sum_{\tau \in T} \left(\sum_{h \in H(\tau)} x_h - 1 \right)^2. \quad (17)$$

The rolling stock continuity constraint from Eq. (3) yields

$$P_2(\vec{y}) = \lambda_2 \left[\sum_{v \in V} \sum_{r \in R} \left(\sum_{h \in H(v)_r^{\text{in}}} k'(h) x_h - \sum_{h \in H(v)_r^{\text{out}}} k(h) x_h \right)^2 + \sum_{v \in V} \left(\sum_{r \in R} \sum_{h \in H(v)_r^{\text{out}}} x_h - s \right)^2 \right] \quad (18)$$

The rolling stock limits in depots from Eq. (4) and (5), yield:

$$P_3(\vec{y}) = \lambda_3 \left[\sum_{d \in D} \sum_{v_d \in V_d} \sum_r \left(\sum_{h \in H(v_d)_r} k'(h) x_h - n(v_d)_r - \sum_{k=1}^{N(v,d)-n(v,d)} s'_k \right)^2 + \sum_{d \in D} \sum_{v'_d \in V'_d} \sum_r \left(\sum_{h \in H(v'_d)_r} k(h) x_h - n'(v'_d)_r - \sum_{k=1}^{N'(v',d)-n'(v',d)} s''_k \right)^2 \right] \quad (19)$$

Capacity constraints for passengers and bicycles imposed in Eqs. (6)–(7), yield:

$$P_4(\vec{y}) = \lambda_4 \left(\sum_{h \in H: p_h > \delta p_h} x_h + \sum_{h \in H: b_h > \delta b_h} x_h \right) \quad (20)$$

Finally the crew constraint in Eq. (8) yields:

$$P_5(\vec{y}) = \lambda_5 \sum_{d \in D} \sum_{t \in \{t_1, t_2, t_3, t_4, \dots\}} \left(\sum_{h \in H(t, d)} k(h)x_h - a(t, d) - \sum_{k=1}^{A(t, d) - a(t, d)} s_k''' \right)^2. \quad (21)$$

In Eqs. (18), (19) and (21) we use slack variables $s, s', s'', s''' \in \{0, 1\}$ to reflect inequalities in Eqs. (3), (4), (5) and (8).

Optionally, the constraint in Eq. (10) can be encoded in a similar way using additional slack variables.

Using the QUBO encoding, the overhead in the number of variables (compared with the ILP scaling in Eq. (13)) is entirely due to the slack variables, since all ILP decision variables are already binary:

$$|\vec{y}| = |\vec{x}| + \#\text{slack vars} \quad (22)$$

Denoting total number of EMUs as $\#EMUs$, $|T|$ as number of trains, and $|D|$ as number of stations - the number of slack variables can be bounded from above by $2N$ (where $N = \max_{v, d} N(v, d) \leq \#EMUs$ is the number of rolling stock in depots) from Eq. (19) and $\#crew \cdot \{t_1, t_2, t_3, t_4, \dots\}$ from Eq. (21), and $|T| \cdot |D|$ from Eq. (18) namely:

$$\#\text{slack vars} \leq 2\#EMUs + \#crew \cdot \{t_1, t_2, t_3, t_4, \dots\} + |T| \cdot |D| \quad (23)$$

In practice, in our instances the number of slack variables is small compared with the number of decision variables.

Regarding the number of QUBO terms, we obtain the following bounds:

- from Eq. (17) if we bound $|H(\tau)|$ via Eq. (11), we have:

$$\#\text{terms} \leq |T| |H(\tau)|^2 = |T|^5 |R|^2 \quad (24)$$

- from Eq. (18) if we bound $|H|(v)_r^{in}|, |H|(v)_r^{out}| \leq 2|R||T|^2$ (the square is from possible joining) and $|V| \leq 2\#(EMUtypes)|T|$ then:

$$\#\text{terms} \leq 2|R||T| (|R||T|^2)^2 \quad (25)$$

In practice, for each node v and EMU type r we limit the number of trains that arcs can start from or lead to, so that $|H(\tau)|, |H|(v)_r^{in}|$ and $|H|(v)_r^{out}|$ can be reduced by the parameters δ and Δ .

- From Eq (19), if we assume that the number of trips leaving depots is at most $|T|$, we obtain

$$\#terms \leq 2|R||T|(2|R||T| + N)^2 \quad (26)$$

where $N = \max_{v,d} N(v,d) \leq \#EMUs$ is the number of rolling stock in depots.

- Eq. (20) yields a bound of the same order as Eq. (6) (7).
- From Eq. (21)

$$\#terms \leq |D||\{t_1, t_2, t_3, t_4, \dots\}|(2|R||T| + A)^2 \quad (27)$$

where $A = \max_{t,d} A(t,d)$ is the number of drivers.

Concluding, the number of QUBO terms scales in the worst case as $|R|^3$ and $|T|^5$, which is problematic when the number of rolling stock types is large. Hence, it is worth examining the frontier of problem sizes that can still be effectively transformed to QUBO, in order to design future hybrid approaches.

3 Solution of the actual problem

The goal is to obtain feasible solutions with practical significance, such that the dispatcher will be able to use them in practice. Additionally, having access to a spectrum of feasible solutions allows the dispatcher to choose one, especially taking into account non-encoded conditions. We use two encodings of the problem,

- an ILP encoding, which is native to the various families of linear solvers that represent the state of the art;
- a QUBO encoding, native for quantum annealers and various quantum-inspired techniques.

To demonstrate the frontier of problem sizes, we solve QUBO using both quantum annealing and quantum-inspired approaches.

Quantum annealing [28, 29] is a heuristic algorithm that runs in the framework of adiabatic quantum computing (AQC) [30], targeting optimization problems. In AQC, a system starting in the lowest energy state (ground state) of some initial Hamiltonian H_0 (a mathematical operator that describes the system's energy) is likely to remain in the ground state throughout the evolution, provided that the system is evolved slowly enough. Hence, if a problem Hamiltonian H_P is introduced gradually, the system is expected to end up in the ground state of H_P at the end of the evolution time T .

Mathematically, the evolution of the system is often described by the time-dependent Hamiltonian

$$H(t) = \left(1 - \frac{t}{T}\right) H_0 + \frac{t}{T} H_P. \quad (28)$$

or, more generally:

$$H(t) = f\left(\frac{t}{T}\right) H_0 + f\left(\frac{t}{T}\right) H_P. \quad (29)$$

where f is the custom “protocol” function, selected in our case to be a linear function.

The quantum annealers provided by D-Wave implement a problem Hamiltonian whose energy is expressed using a 2-local Ising model [31]:

$$H_P = \sum_{i,j \in \mathcal{E}} J_{ij} \sigma_i^z \sigma_j^z + \sum_i h_i \sigma_i^z, \quad (30)$$

where σ^z is a Pauli- Z operator acting on the i -th qubit, and J_{ij} and h_i are real values corresponding to pairwise couplings and the external magnetic field, respectively. The set \mathcal{E} represents the processor graph, i.e., the connectivity graph of a particular quantum device. However, the connectivity of quantum hardware often differs from the connectivity required by the optimization problem. To handle this mismatch, a minor embedding is required to translate the problem topology onto the processor topology [32]. In the D-Wave implementation, one chooses H_0 to consist of a transverse magnetic field:

$$H_0 = h_0 \sum_i \sigma_i^x \quad (31)$$

where σ_i^x is the Pauli- X operator acting on the i -th qubit.

To see why the QUBO representation in Eqs. (16) - (21) can be implemented straightforwardly on a quantum annealer, observe that a binary variable y_i can be easily transformed into a spin variable $s_i \in \{-1, 1\}$ via $y_i = \frac{s_i + 1}{2}$ [31]. Substituting this into Eq. (14) yields the following optimization problem:

$$\min_{\vec{s}} \left(\sum_{i < j} J_{i,j} s_i s_j + \sum_i h_i s_i \right). \quad (32)$$

Following [33], such a formulation is supposed to be minimized if corresponding to the minimal energy state of the quantum Hamiltonian in Eq. (30).

A potential alternative direction in solving QUBOs is the application of quantum-inspired algorithms [34]. Following this path, we apply the new VeloxQ solver [22], which appears to be effective for large, sparse QUBOs (with a limited number of connections) [25, 24, 26, 23]. This heuristic solver

takes a QUBO or Ising instance and returns a series of solutions intended to originate from the problem’s low-energy spectrum (hopefully including at least one feasible solution). VeloxQ is a physics-inspired classical solver for QUBO/Ising problems that mimics energy-minimization dynamics without requiring quantum hardware and achieve high scalability on standard CPUs/GPUs. Compared to D-Wave quantum annealing and simulated bifurcation, it delivers comparable or superior solution quality and runtime, especially for large, arbitrarily connected problem instances.

3.1 Toy model

The toy model is defined by the timetable $T = \{\tau_1, \tau_2, \tau_3\}$ where τ_1 and τ_2 are trains that go $A \rightarrow B$, and τ_3 goes $B \rightarrow A$. The timetable is arranged so that any rolling stock that arrives at B can either remain there or return to A . Two EMU types $R = \{r_1, r_2\}$ are available at the depot at station A throughout the time horizon, with fleet sizes $N(v_d)_{r_1} = 2, N(v_d)_{r_2} = 1$ with the seats capacity $p_1 = 70, p_2 = 110$. There is also an optional service train v_4 going from B to A (which can be served only by type r_1). We assume that $A = 2$ drivers are available throughout the horizon; they can drive any of the two EMUs and take any of the trips. Finally, we do not consider bicycles in this example.

We assume the following costs:

- operating costs of EMUs (the same on both trips): $r_1 - 70, r_2 - 110$ (we assume these costs are additive);
- expected numbers of passengers on the trips: $\tau_1 - 70, \tau_2 - 60, \tau_3 - 100$,

For this example we assume that the number of passengers is constant over each trip and that the seat shortage cannot exceed $\delta p_h = 10$ for a single EMU and $\delta p_h = 20$ for coupled EMUs. Let us also assume that EMUs can not be coupled at station A , but they can be coupled at station B and only type r_1 is allowed to form coupled compositions.

The hyper-graph of the problem is composed of the following nodes: $V = \{v_d, v_1, v_2, v_3, v_4\}$ where v_d represents service trains from the depot that are not included in timetable and v_4 represents the optional service train. Let

$$\begin{aligned} H = & \{h_{v_d, v_1, r_1}, h_{v_d, v_1, r_2}, h_{v_d, v_2, r_1}, h_{v_d, v_2, r_2}, h_{v_1, v_3, r_1}, h_{v_1, v_3, r_2}, h_{v_1, v_4, r_1}, \\ & h_{v_2, v_3, r_1}, h_{v_2, v_3, r_2}, h_{v_2, v_4, r_1}, h_{(v_1, v_2), (v_3, v_3), r_1}\} \\ \Rightarrow & \{x_0, x_1, \dots, x_8, x_9, x_{10}\} \end{aligned} \quad (33)$$

where the variable x_{10} corresponds to the hyper-arc $h_{(v_1, v_2), (v_3, v_3), r_1}$ that represents coupling two EMUs at station B .

We then have

$$H(v_1)^{\text{in}} = \{h_{v_d, v_1, r_1}, h_{v_d, v_1, r_2}\}, \quad H(v_2)^{\text{in}} = \{h_{v_d, v_2, r_1}, h_{v_d, v_2, r_2}\} \Rightarrow \{0, 1\} \{2, 3\} \quad (34)$$

and

$$\begin{aligned} H(v_1)^{\text{out}} &= \{h_{v_1, v_3, r_1}, h_{v_1, v_3, r_2}, h_{v_1, v_4, r_1}, h_{(v_1, v_2), (v_3, v_3), r_1}\}, \\ H(v_2)^{\text{out}} &= \{h_{v_2, v_3, r_1}, h_{v_2, v_3, r_2}, h_{v_2, v_4, r_1}, h_{(v_1, v_2), (v_3, v_3), r_1}\} \\ &\Rightarrow \{4, 5, 6, 10\} \{7, 8, 9, 10\} \end{aligned} \quad (35)$$

while

$$\begin{aligned} H(v_d)_{r=1} &= \{h_{v_d, v_1, r_1}, h_{v_d, v_2, r_1}\} \text{ and } H(v_d)_{r=2} = \\ &\{h_{v_d, v_1, r_2}, h_{v_d, v_2, r_2}\} \Rightarrow \{0, 2\} \{1, 3\} \end{aligned} \quad (36)$$

and

$$\begin{aligned} H(\tau_1) &= \{h_{v_d, v_1, r_1}, h_{v_d, v_1, r_2}\}, \quad H(\tau_2) = \{h_{v_d, v_2, r_1}, h_{v_d, v_2, r_2}\} \Rightarrow \{0, 1\} \{2, 3\} \\ H(\tau_3) &= \{h_{v_1, v_3, r_1}, h_{v_1, v_3, r_2}, h_{v_2, v_3, r_1}, h_{v_2, v_3, r_2}, h_{(v_1, v_2), (v_3, v_3), r_1}\} \Rightarrow \{4, 5, 7, 8, 10\}. \end{aligned} \quad (37)$$

Proposed ILP Assume $\alpha = 0.01$. The objective becomes:

$$\begin{aligned} \min_{\vec{x}} &\left(\alpha \sum_{h \in H} c_h x_h + \sum_{r \in \{r_1, r_2\}} \sum_{h \in H(v_d)_r} k(h) x_h \right) \\ &= \left(0.7x_0 + 1.1x_1 + 0.7x_2 + 1.1x_3 + 0.7x_4 + \right. \\ &\quad \left. 1.1x_5 + 0.7x_6 + 0.7x_7 + 1.1x_8 + 0.7x_9 + 1.4x_{10} \right) + \\ &\quad (1x_0 + 1x_1 + 1x_2 + 1x_3) \end{aligned} \quad (38)$$

The coverage constraint in Eq. (2) would be:

$$\begin{aligned} \forall \tau \in T \quad \sum_{h \in H(\tau)} x_h &= 1 \\ x_0 + x_1 &= 1 \quad x_2 + x_3 = 1, \quad x_4 + x_5 + x_7 + x_8 + x_{10} = 1 \end{aligned} \quad (39)$$

The continuity constraint in Eq. (3) are:

$$\begin{aligned} \sum_{h \in H(v)_r^{\text{in}}} k'(h) x_h &= \sum_{h \in H(v)_r^{\text{out}}} k(h) x_h, \quad \forall v \in \{v_1, v_2\} r \in \{r_1, r_2\} \end{aligned} \quad (40)$$

$$\begin{aligned} (\text{for } v_1) \quad x_0 &= x_4 + x_6 + x_{10} \text{ and } x_1 = x_5 \quad (\text{for } v_2) \quad x_2 = x_7 + x_{10} + \\ &x_9 \text{ and } x_3 = x_8 \end{aligned} \quad (41)$$

and

$$\forall v \in \{v_1, v_2\} \quad \sum_{r \in \{r_1, r_2\}} \sum_{h \in H(v)_r^{\text{out}}} x_h \leq 1 \quad (42)$$

$$x_{10} + x_4 + x_5 + x_6 \leq 1 \quad x_{10} + x_7 + x_8 + x_9 \leq 1 \quad (43)$$

Depot constraint Eq. (4) (we drop the return constraints in Eq. (5)) reduce to

$$\sum_{h \in H(v_d)_r} k(h)x_h \leq N(v_d)_r, \quad \forall v_d \in \{v_d\} \forall r \in \{r_1, r_2\}$$

$$x_0 + x_2 \leq 2 \quad x_1 + x_3 \leq 1 \quad (44)$$

Concerning capacity (seats) constraint

$$\sum_{h \in H: p_h > \delta p_h} x_h = 0, \quad (45)$$

$$x_4 + x_7 = 0 \quad (46)$$

Other capacity constraints for this model are trivial, hence not included. For the driver's constraint, let us assume that

$$H(t_1, d) = \{h_{v_d, v_1, r_1}, h_{v_d, v_1, r_2}\} \quad A(t_1, d) = 2 \quad (47)$$

$$H(t_2, d) = \{h_{v_1, v_3, r_1}, h_{v_1, v_3, r_2}, h_{v_1, v_4, r_2}, h_{v_2, v_3, r_1}, h_{v_2, v_3, r_2}, h_{v_2, v_4, r_2},$$

$$h_{(v_1, v_2), (v_3, v_3), r_1}\} \quad A(t_2, d) = 2 \quad (48)$$

yielding

$$\forall d \in D \forall (t) \in \{t_1, t_2\} \quad \sum_{h \in H(t, d)} x_h \leq A(t, d) \quad (49)$$

$$x_0 + x_1 \leq 2 \quad (50)$$

$$x_4 + x_5 + x_6 + x_7 + x_8 + x_9 + x_{10} \leq 2 \quad (51)$$

We obtain the optimal solution $x_0 = 1, x_2 = 1, x_{10} = 1$ with $f(\vec{x}) = 4.80$. The corresponding network structure is shown in Fig. 3. We also identify two feasible excited solutions:

- $x_0 = 1, x_3 = 1, x_6 = 1, x_8 = 1$ with $f(\vec{x}) = 5.6$
- $x_1 = 1, x_2 = 1, x_5 = 1, x_9 = 1$ with $f(\vec{x}) = 5.6$

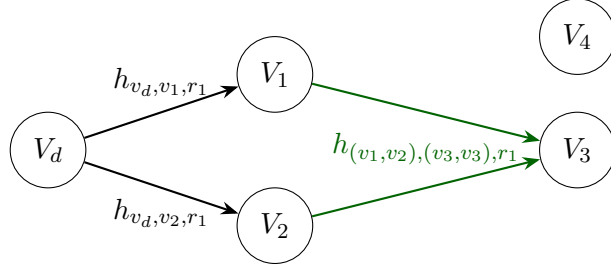


Figure 3: Illustration of the network structure of the optimal solution of the toy problem. Black arrows represent arcs, while green arrows represent the single hyper-arc.

Proposed QUBO We convert the ILP problem into the QUBO using the penalty method, i.e., by adding quadratic penalty terms corresponding to Eqs. (16)- (20) and Eq. (21). Then the resulting QUBO objective is:

$$\begin{aligned} \min_{\vec{x}} : \\ 1.7x_0 + 2.1x_1 + 1.7x_2 + 2.1x_3 + 0.7x_4 + 1.1x_5 + 0.7x_6 + 0.7x_7 + 1.1x_8 + \\ 0.7x_9 + 1.4x_{10} + \end{aligned} \quad (52)$$

$$\lambda_1 \left((x_0 + x_1 - 1)^2 + (x_2 + x_3 - 1)^2 + (x_4 + x_5 + x_7 + x_8 + x_{10} - 1)^2 \right) + \quad (53)$$

$$\begin{aligned} \lambda_2 \left((x_4 + x_6 + x_{10} - x_0)^2 + (x_5 - x_1)^2 + (x_7 + x_9 + x_{10} - x_2)^2 + (x_8 - x_3)^2 + \right. \\ \left. (x_4 + x_5 + x_6 + x_{10} - s_{11})^2 + (x_7 + x_8 + x_9 + x_{10} - s_{12})^2 \right) + \end{aligned} \quad (54)$$

$$\lambda_3 \left((x_0 + x_2 - s_{13} - s_{14})^2 + (x_1 + x_3 - s_{15})^2 \right) + \quad (55)$$

$$\lambda_4 (x_4 + x_7) + \quad (56)$$

$$\lambda_5 \left((x_0 + x_1 - s_{16} - s_{17})^2 + (x_4 + x_5 + x_6 + x_7 + x_8 + x_9 + x_{10} - s_{18} - s_{19})^2 \right) \quad (57)$$

where $s_i \in \{0, 1\}$ are slack variables used to encode the inequality constraints.

An interesting feature of this formulation is that, if we set λ_4 small relative to the other penalty coefficients, solutions that violate only the seat capacity constraint (i.e., that corresponds to overcrowded trains) may still appear among low-energy states, while all other constraints remain satisfied.

In the toy example, we used the D-Wave simulator with $\lambda_1 = \lambda_2 = \lambda_3 = \lambda_4 = \lambda_5 = 100$ for the reason mentioned above. With this choice we obtain the following set of low-energy solutions, both feasible and non-feasible:

- Optimum: $x_0 = 1, x_2 = 1, x_{10} = 1$ and $f(\vec{x}) = 4.8$

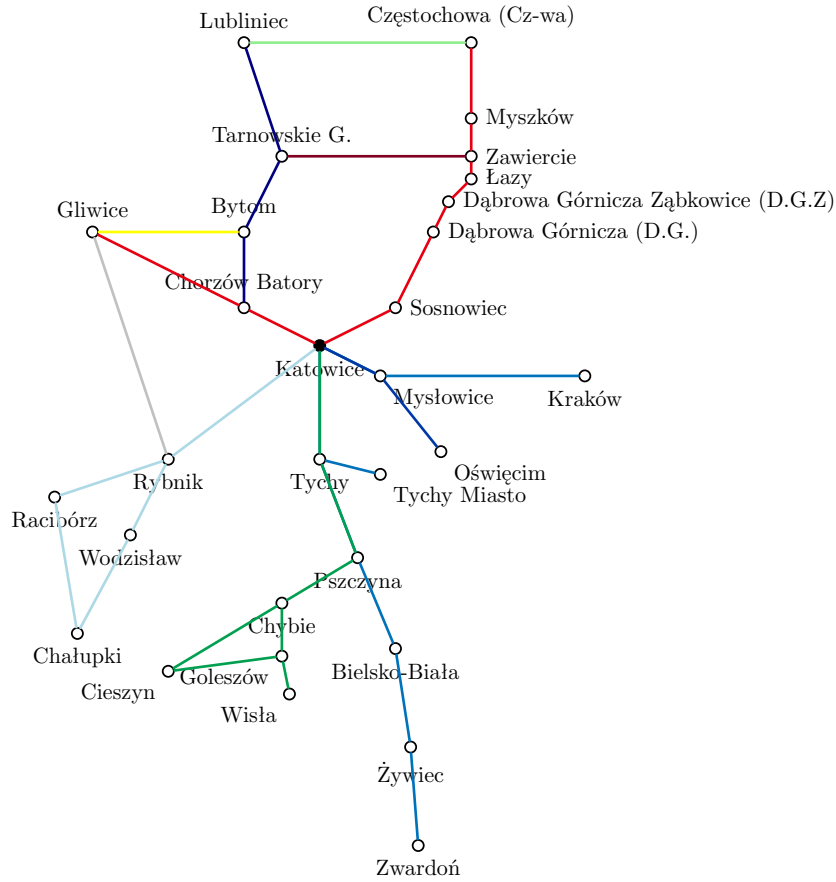


Figure 4: Schematic topology of the network, for the more detailed one see https://www.kolejeslaskie.com/rozklad_jazdy/schemat-linii-komunikacyjnych/

- $x_0 = 1, x_3 = 1, x_6 = 1, x_8 = 1$ and $f(\vec{x}) = 5.6$
- $x_1 = 1, x_2 = 1, x_5 = 1, x_9 = 1$ and $f(\vec{x}) = 5.6$
- Not feasible (capacity) $x_0 = 1, x_2 = 1, x_6 = 1, x_7 = 1$
- Not feasible (capacity) $x_1 = 1, x_2 = 1, x_4 = 1, x_9 = 1$

3.2 Practical problems

We test our model on practical instances of various sizes, constructed from real-life timetables of the Silesian region in Poland. The instances correspond to daily rolling stock schedules on networks of gradually increasing size.

To schedule rolling stock, we use the actual timetable from December 2024 supplied by the partner (Koleje Śląskie). Beyond the toy model from Section 3.1, the smallest practical instance (instances 1 and 1 a) concerns the daily traffic between two neighbouring stations, Gliwice and Bytom. Subsequent instances gradually increase the size of the considered network, namely:

- 2 2 a) — Gliwice–Bytom, Gliwice–Rybnik and Rybnik–Racibórz,
- 3, 4, 4 a) — Gliwice–Częstochowa and intermediate stations (case 3 has limited *Delta* parameter values),
- 5, 5 a) — as in cases 4, 4 a) and Gliwice–Bytom and Gliwice–Rybnik
- 6, 6 a) — as in cases 5, 5 a) and Częstochowa–Tarnowskie Góry.

The largest instances (7, 7 a) and 8, 8 a) concern traffic across almost the entire network, with some limitations due to data availability (Częstochowa–Lubliniec) and limited train service caused by engineering works (Żywiec–Zwardoń). Cases 8 and 8 a) use enlarged Δ parameter value.

For most of the above base instances there exist corresponding variants with increased passenger and bicycle demand, denoted by 'a)'. Finally, since we consider daily rolling stock circulation plans, we consider as depots central stations (such as Gliwice, Katowice, and Częstochowa) as well as terminal (edge) stations, where trains start their routes in the morning and/or end in the evening. This is a new interesting aspect in our model, enabling the use of daily schedules in the practical application of rescheduling or as part of a larger multi-day model.

The specifics and sizes of all instances are presented in Tab. 2.

inst.	$ T $	$ T' / T'' $	$ D $	$ R $	δ	Δ	# ILP vars	# QUBO vars / terms
toy	3	2/1	1	2	10	60	11	20/ 88
1	30	30/0	1	1	5	60	33	42/ 93
1a	30	0/30	1	1	5	60	66	103 / 371
2	51	51/0	3	1	5	60	74	103 / 309
2a	51	21/30	3	1	5	60	120	172 / 800
3	78	30/48	6	5	5	60 - 150	1599	1756 / 87121
4	78	30/48	6	5	5	300	6238	6295 / $1.8 \cdot 10^6$
4a	78	30/48	6	5	5	300	6238	6295 / $1.8 \cdot 10^6$
5	126	78/48	7	11	5	300	$4.8 \cdot 10^4$	$4.8 \cdot 10^4 / 8.5 \cdot 10^7$
5a	126	78/48	7	11	5	300	$4.8 \cdot 10^4$	$4.8 \cdot 10^4 / 8.5 \cdot 10^7$
6	143	95/48	8	11	5	300	$5.2 \cdot 10^4$	$5.2 \cdot 10^4 / 9.8 \cdot 10^7$
6a	143	95/48	8	11	5	300	$5.2 \cdot 10^4$	$5.2 \cdot 10^4 / 9.8 \cdot 10^7$
7	404	356/48	19	11	5	300	$8.2 \cdot 10^4$	$8.3 \cdot 10^4 / 1.5 \cdot 10^8$
7a	404	356/48	19	11	5	300	$8.2 \cdot 10^4$	$8.3 \cdot 10^4 / 1.5 \cdot 10^8$
8	404	356/48	19	11	5	960	$3.8 \cdot 10^5$	n.a.
8a	404	356/48	19	11	5	960	$3.8 \cdot 10^5$	n.a.

Table 2: Instance descriptions. Instances marked by a) have increased passenger and bicycle demand. For large instances number of QUBO variables is similar to the number of ILP variables (the impact of slack variables is limited), but the size of the QUBO in terms of its terms grows rapidly. The largest QUBOs could not be constructed due to the memory limits of the 62 GB RAM. (Recall that T' are trips that can be served only by the single EMU, while T'' are trips that can be served by either single or multiple EMUs.)

inst.	$\alpha = 0.01$		$\alpha = 0.0001$		$\alpha = 0.0$	
	comp time [s]	objective	comp time [s]	objective	comp time [s]	objective
toy	0	4.8	0	2.03	0	2.0
1	0	110.66	0	2.10	0	1.0
1a	0	119.71	0	3.18	0	2.0
2	0	251.38	0	5.48	0	3.0
2a	0	260.44	0	6.56	0	4.0
3	0.29	2037.85	0.30	36.22	0.91	16.0
4	2.17	1817.56	3.23	33.76	5.44	15.0
4a	1.88	1843.56	1.89	34.59	4.63	16.0
5	23.76	2060.87	26.23	39.79	55.61	19.0
5a	22.47	2073.86	22.61	39.91	55.88	19.0
6	37.89	2404.10	31.15	44.31	31.50	20.0
6a	33.14	2416.53	28.05	44.55	61.99	20.0
7	378.37	4852.04	153.10	92.18	1137.89	43.0
7a	278.28	4853.11	102.45	92.26	911.95	43.0
8	250.28	4759.22	698.92	92.09	2257.09	43.0
8a	209.00	4759.22	336.71	92.17	4852.04	43.0

Table 3: ILP solutions of the SCIP solver *version 9.2.1*. Computational time rounded to 0.01 s. Comparing cases 7, 7 a) with 8, 8 a) one can conclude that heuristic limitations of the Δ parameter reduce the computational time at a relatively small cost in the objective value. The computations were performed on 13th Gen Intel(R) Core(TM) i5-1340P @4 GHz, 12 cores, 16 threads.

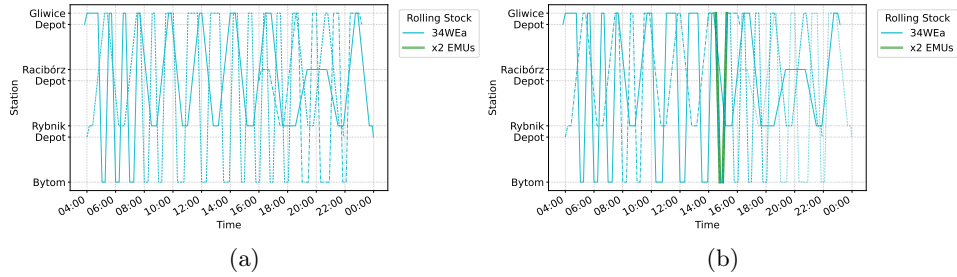


Figure 5: Train diagrams of ILP solutions of the following instances 2 (left) and 2a (right). The green line means two rolling pieces of stock coupled. We use $\alpha = 0.01$ in Eqs. (1)–(9).

ILP solutions using the SCIP solver *version 9.2.1* [35, 36] for these instances are presented in the Table 3. Train diagrams for selected instances are presented in Fig. 5, Fig. 6.

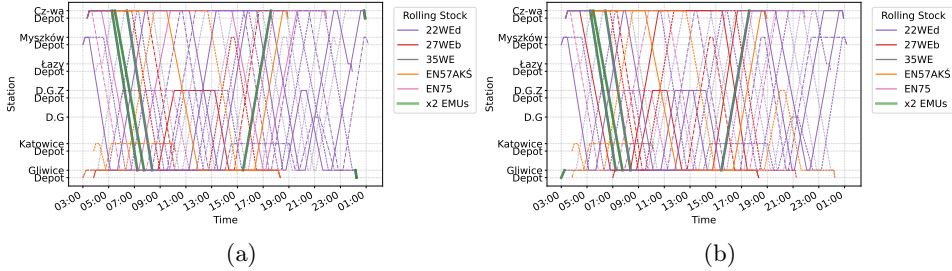


Figure 6: Train diagrams of ILP solutions of the following and 4 (left) and 4a (right). Different colors represent different types of rolling stock. The green line means two rolling pieces of stock coupled. We use $\alpha = 0.01$ in Eqs. (1)–(9).

The results of quantum annealing on the D-Wave machine are presented in Fig 7.

Although the quantum annealing approach is currently applicable only to small instances and does not outperform the ILP approach in terms of computational time, there is clear progress in quantum annealing technology developments when comparing the older `Advantage_system6.4` with the newer `Advantage2_system1.7` [37]. In the first case, only the simplest instances (toy, 1, 2) were solvable, while `Advantage2_system1.7` allowed us to solve more complex ones, i.e., 1a and 2a.

The `Advantage_system6.4` uses the Pegasus topology (with ~ 15 -way connectivity) and has about 5,612 qubits, while the `Advantage2_system1.7` uses the newer Zephyr topology with 20-way connectivity, enabling more compact embeddings. Advantage2 also has a higher energy scale, lower noise, and about twice the qubit coherence time, which together improve solution quality and speed [38] [37]. For various feasible solutions from quantum annealing, see the example on the toy model in Fig. 8.

Results obtained with the quantum-inspired VeloxQ solver [22] are presented in Fig. 9. We observe better performance than D-Wave for small instances; however, large instances were not tractable with this approach. Although the VeloxQ achieves better results than D-Wave, the performance gap remains moderate when compared with the classical ILP approach.

4 Discussion

We examined daily rolling stock circulation planning for EMUs under operational constraints relevant to the Silesian Railway operator, including (i) limited, predefined coupling of identical units in pairs, and (ii) demand-driven capacity requirements for both seats and bicycle spaces. Using real timetable-based instances of increasing size, we compared a classical ILP

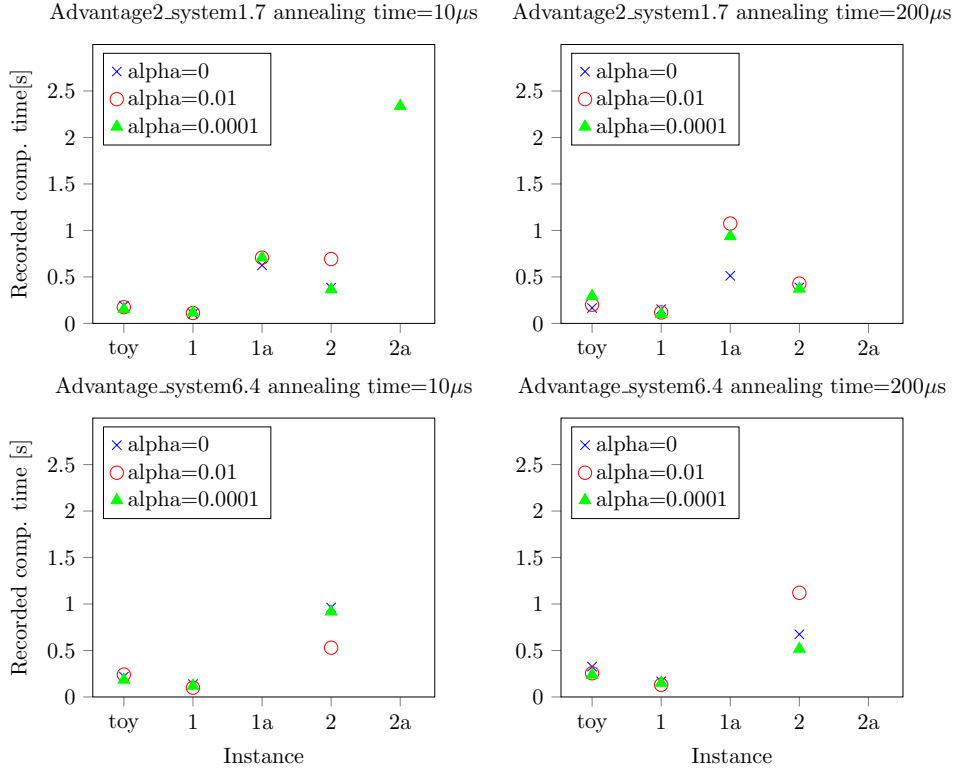


Figure 7: Results of the D-Wave experiments. We report the computation time (minor embedding time, network/queue latency, QPU sampling time, embedding processing) for each instance together with the required number of runs to reach the optimal solution (we start with 100 runs on D-Wave and increase it gradually if the optimal solution is not found). In the 2a instance, we obtained, for one parameter setting, a solution that is optimal for the original problem but does not satisfy the constraints on the slack variables in the QUBO encoding. Instance 3 was too large to be embedded and thus could not be run on the D-Wave machine. If there is no record, we were unable to reach a feasible solution, within 5000 runs of $10\mu\text{s}$ of annealing time or 2500 runs of $200\mu\text{s}$ of annealing time. The D-Wave QPU was accessed through a 13th Gen Intel Core i7-13700HX with 24 threads and 64GB of RAM.

approach against QUBO-based solution paradigms—quantum annealing on D-Wave and the quantum-inspired VeloxQ solver—to empirically characterize where QUBO methods are currently tractable for this application.

For the tested daily instances, the classical ILP formulation can produce feasible circulation plans at practical computational cost across the full range of instance sizes considered. In particular, the ILP solves instances up to 404 trips and 11 EMU types (instances 7/7a/8/8a in Table (2)) with runtimes

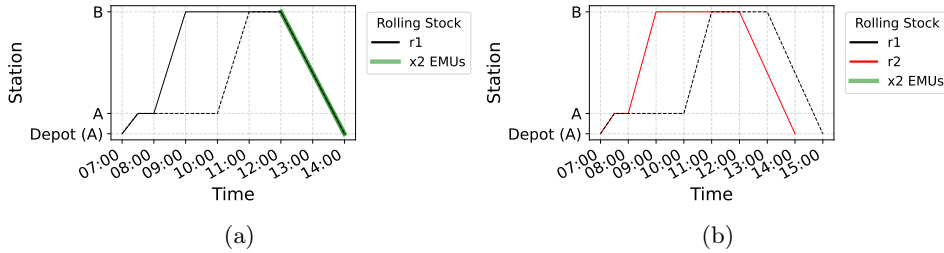


Figure 8: Two D-Wave Advantage2_system1.7 solutions of the toy case: left, the ground state with objective 4.8; right, an excited state with objective value 5.6

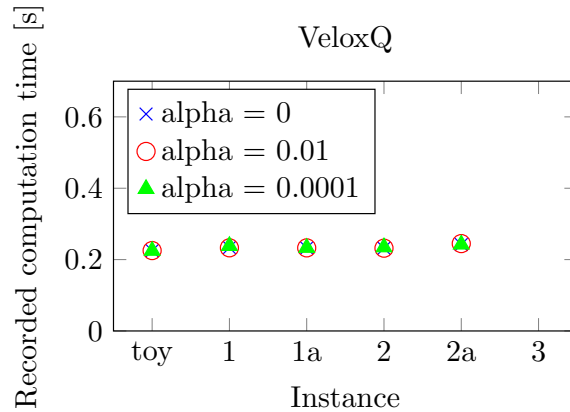


Figure 9: Results of the VeloxQ experiments [22], computational time on VeloxQ solver, all results were feasible and optimal, we used the default setting for instances (toy, 1, 1a, 2, 2a). The computations were performed on 13th Gen Intel(R) Core(TM) i5-1340P @4 GHz, 12 cores, 16 threads.

ranging from sub-second on small cases to tens of minutes on the largest cases depending on the objective weighting α (Table (3))

A practically relevant observation is that limiting the maximum transfer window Δ —used as a heuristic to cap arc generation and thus reduce model density—can reduce solution time substantially with only a relatively small loss in objective value. This is visible when comparing cases 7/7a ($\Delta = 300$) with 8/8a ($\Delta = 960$) and is explicitly noted in the Table (3) caption. From an operational perspective, this supports a two-mode workflow: (i) a fast “restricted- Δ ” solve to obtain a high-quality plan quickly during disruptions, and (ii) an optional refinement step (larger Δ) when additional computation time is available.

Across the tested instances, the dominant barrier for direct QUBO-based/Ising approaches is not the number of binary variables per se, but the

quadratic expansion and connectivity/embedding overhead. In the larger instances, the number of QUBO variables remains close to the number of ILP variables (slack-variable overhead is limited), yet the number of QUBO terms grows rapidly, reaching $\sim 1.5 \times 10^8$ terms in instance 7/7a, and QUBO construction becomes infeasible for the largest Δ cases (8/8a) under the available 62 GB RAM. This practical bottleneck is consistent with the scaling discussion of the QUBO term count and with the observation that problem sparsification via tighter δ/Δ windows is essential to keep QUBOs manageable.

On D-Wave, quantum annealing is currently applicable only to the smallest instances considered. Instance 3 was already too large to embed, and for some settings (e.g., instance 2a), the sampler may return a solution that is optimal for the original objective but violates slack-variable constraints in the QUBO encoding—highlighting the sensitivity to penalty calibration and the need for systematic feasibility screening when using penalty-based formulations. At the same time, the comparison between hardware generations indicates tangible progress: the older Advantage_system6.4 could solve only the simplest cases (toy, 1, 2), while Advantage2_system1.7 enabled additional instances (1a and 2a for some parameter settings). For the VeloxQ solver, results are stronger than D-Wave on small cases and were feasible and optimal for instances up to instance 3 under the default configuration; however, larger instances were still not tractable in this direct QUBO approach, and the remaining gap versus ILP remains substantial for practical deployment.

A key requirement from practice is not only to obtain one feasible plan, but to have multiple feasible alternatives available quickly so that dispatchers can account for non-modelled considerations and coordinate with infrastructure management. The toy example illustrates that the model naturally admits multiple feasible “excited” solutions beyond the optimum. This feature aligns well with the behavior of annealing-based approaches, which aim to sample from low-energy regions rather than output a single deterministic solution; in principle, this could be operationally valuable when a DSS needs to offer a small portfolio of near-optimal circulation options (e.g., different reserve usage levels, different coupling choices, or different depot return patterns) under time pressure. However, the experiments also show that obtaining a useful portfolio of feasible solutions from QUBO samplers requires careful constraint encoding (penalty design), feasibility checks, and likely post-processing—otherwise low-energy samples can still violate critical constraints (e.g., slack-variable feasibility).

Taken together, the results suggest a clear division of labor for near-term methods:

- **Classical ILP** is currently the most reliable approach for end-to-end daily circulation planning at the tested scales (hundreds of trips, many

depots, and many rolling-stock types).

- **QUBO-based Quantum and quantum-inspired** are presently most suitable as subproblem optimizers on carefully bounded instances (few rolling stock types, limited trip subsets, limited time windows), consistent with the limitations observed in embedding and QUBO construction.

This points toward hybrid architectures in which the full daily problem is solved classically, while QUBO-based optimization is applied selectively to localized, high-impact decisions. Concretely, promising decomposition directions include:

- Local spatio-temporal neighborhoods around a disruption (e.g., the next 1–3 hours and a small corridor), where only a small set of trips and feasible turnarounds matter.
- Coupling/decoupling “hotspots” (stations and predefined coupling trips), where composition decisions create combinatorial difficulty but remain geographically and temporally localized.
- Type-restricted subproblems (a few EMU types relevant to the disrupted lines), which directly attack the observed $|R|$ (i.e. number of types of EMUs) sensitivity in QUBO term growth.

In such a hybrid approach, the quantum layer would not replace the ILP solver; rather, it would complement it by rapidly exploring alternative local rewirings (and producing multiple candidate solutions) while the classical layer maintains global feasibility and overall resource balance.

While daily (acyclic) planning appears tractable with classical solvers, extending to multi-day circulation introduces additional complexity that can quickly exceed straightforward daily formulations. The appendix sketches one potential direction inspired by column generation: start from daily schedules that begin/end in depots, then add variables that allow overnight transfers to join daily schedules into more efficient multi-day rotations under practical feasibility constraints. Developing this direction further—together with maintenance constraints, richer crew constraints, and disruption scenarios beyond demand surges—would provide a natural next step for both classical and hybrid solution approaches.

Finally, we note several limitations that motivate future work. The coupling policy is intentionally restricted (pairs of identical EMUs and only on predefined trips), which matches the partner’s operational practice but reduces flexibility. For QUBO-based methods, the study relies on penalty-based encodings and therefore inherits typical challenges of penalty selection, feasibility screening, and quadratic expansion; addressing these issues—e.g.,

by tighter formulations, structured decompositions, and systematic calibration—appears necessary before QUBO methods can be considered for larger real-world circulation instances.

Acknowledgements

The authors acknowledge the cooperation with the railway operator Koleje Śląskie sp. z o.o, in particular concerning the problem statement, data acquisition, and discussion on results. The authors acknowledge the Jülich Supercomputing Centre for providing computing time on the D-Wave Advantage™ System JUPSI through the Jülich UNified Infrastructure for Quantum computing (JUNIQ).

Z.M. acknowledges funding from the Ministry of Economic Affairs, Labour and Tourism Baden-Württemberg in the frame of the Competence Center Quantum Computing Baden-Württemberg (project “KQCBW25”)

K.D. acknowledges: Scientific work co-financed from the state budget under the program of the Minister of Education and Science, Poland (pl. Polska) under the name "Science for Society II" project number NdS-II/SP/0336/2024/01 funding amount 1000000 PLN total value of the project 1000000 PLN 

We appreciate the assistance of Peter Márton - University of Žilina, Department of Mathematical Methods and Operations Research, Faculty of Management Science and Informatics - on discussing the railway model and feedback on the manuscript.

Appendix - A

Potential multi-day EMUs circulation plan Although we concentrate on the operational reaction to usual events, our model can be modified for the multi-day circulation plans. Here, our partner limits himself to a rather short few-day schedule with a limit of say 5 days. To solve such a problem, inspired by the column generation approach [39], in terms of adding new variables to join one-day schedules.

- We start with the sequence of one-day schedules where all trains have one-day trips starting and ending in dedicated depots.
- Then we create new variables that allow for the transfer of the rolling stock overnight in some chosen locations, joining one-day schedules into the multi-day ones that are more effective (e.g., in terms of used rolling stock)
- to select the new variables, we use the subset of operation points satisfying the partner’s requirements and the technical feasibility of staying of rolling stock overnight.

References

- [1] B. Tan, M.-A. Lemonde, S. Thanasilp, J. Tangpanitanon, D. G. Angelakis, Qubit-efficient encoding schemes for binary optimisation problems, *Quantum* 5 (2021) 454. doi:10.22331/q-2021-05-04-454.
- [2] L. Lamorgese, C. Mannino, D. Pacciarelli, J. T. Krasemann, Train dispatching (2018) 265–283doi:10.1007/978-3-319-72153-8_12.
- [3] H. Pan, L. Yang, Z. Liang, H. Yang, New exact algorithm for the integrated train timetabling and rolling stock circulation planning problem with stochastic demand, *European Journal of Operational Research* 316 (3) (2024) 906–929. doi:10.1016/j.ejor.2024.02.017.
- [4] P.-J. Fioole, L. Kroon, G. Maróti, A. Schrijver, A rolling stock circulation model for combining and splitting of passenger trains, *European Journal of Operational Research* 174 (2) (2006) 1281–1297. doi:10.1016/j.ejor.2005.03.032.
- [5] H. Zhou, J. Qi, L. Yang, J. Shi, H. Pan, Y. Gao, Joint optimization of train timetabling and rolling stock circulation planning: A novel flexible train composition mode, *Transportation Research Part B: Methodological* 162 (2022) 352–385. doi:10.1016/j.trb.2022.06.007.
- [6] J. L. Espinosa-Aranda, R. García-Ródenas, L. Cadarso, Ángel Marín, Train scheduling and rolling stock assignment in high speed trains, *Procedia - Social and Behavioral Sciences* 160 (2014) 45–54, xI Congreso de Ingeniería del Transporte (CIT 2014). doi:10.1016/j.sbspro.2014.12.115.
- [7] M. Peeters, L. Kroon, Circulation of railway rolling stock: a branch-and-price approach, *Computers & Operations Research* 35 (2) (2008) 538–556. doi:10.1016/j.cor.2006.03.019.
- [8] Y. Wang, A. D’Ariano, J. Yin, L. Meng, T. Tang, B. Ning, Passenger demand oriented train scheduling and rolling stock circulation planning for an urban rail transit line, *Transportation Research Part B: Methodological* 118 (2018) 193–227. doi:10.1016/j.trb.2018.10.006.
- [9] N. Chai, Z. Chen, W. Zhou, Periodic and aperiodic train timetabling and rolling stock circulation planning using an efficient lagrangian relaxation decomposition, *Computers & Operations Research* 180 (2025) 107062. doi:10.1016/j.cor.2025.107062.
- [10] J. Niu, K. Qiao, P. Zhao, Reliability improvement of rolling stock planning with maintenance requirements for high-speed railway, *Reliability Engineering & System Safety* 259 (2025) 110972. doi:10.1016/j.ress.2025.110972.

- [11] Y. Shen, W. Xie, J. Li, Multiobjective optimization approach for integrated timetabling and vehicle scheduling with uncertainty, *Journal of Advanced Transportation* (2020). doi:10.1155/2021/3529984.
- [12] T. Nishi, A. Ohno, M. Inuiguchi, S. Takahashi, K. Ueda, A combined column generation and heuristics for railway short-term rolling stock planning with regular inspection constraints, *Computers & Operations Research* 81 (2017) 14–25. doi:10.1016/j.cor.2016.11.025.
- [13] H. Pan, L. Yang, Z. Liang, Demand-oriented integration optimization of train timetabling and rolling stock circulation planning with flexible train compositions: A column-generation-based approach, *European Journal of Operational Research* 305 (1) (2023) 184–206. doi:10.1016/j.ejor.2022.05.039.
- [14] X. Bao, Q. Zhang, H. Yin, E. Wang, Y. Xiao, Integrated optimization of demand-oriented timetabling and rolling stock circulation planning with flexible train compositions and multiple service routes on urban rail lines, *Transportation Research Part C: Emerging Technologies* 174 (2025) 105071. doi:10.1016/j.trc.2025.105071.
- [15] Y. Gao, J. Xia, A. D’Ariano, L. Yang, Weekly rolling stock planning in chinese high-speed rail networks, *Transportation Research Part B: Methodological* 158 (2022) 295–322. doi:10.1016/j.trb.2022.02.005.
- [16] R. Borndörfer, T. Eßer, P. Frankenberger, A. Huck, C. Jobmann, B. Krostitz, K. Kuchenbecker, K. Mohrhagen, P. Nagl, M. Peterson, et al., Deutsche bahn schedules train rotations using hypergraph optimization, *INFORMS Journal on Applied Analytics* 51 (1) (2021) 42–62. doi:10.1287/inte.2020.1069.
- [17] J. T. Haahr, J. C. Wagenaar, L. P. Veelenturf, L. G. Kroon, A comparison of two exact methods for passenger railway rolling stock (re)scheduling, *Transportation Research Part E: Logistics and Transportation Review* 91 (2016) 15–32. doi:10.1016/j.tre.2016.03.019.
- [18] W. Zhou, Y. Huang, L. Deng, J. Qin, Collaborative optimization of energy-efficient train schedule and train circulation plan for urban rail, *Energy* 263 (2023) 125599. doi:10.1016/j.energy.2022.125599.
- [19] C. Grozea, R. Hans, M. Koch, C. Riehn, A. Wolf, Optimising rolling stock planning including maintenance with constraint programming and quantum annealing, *arXiv preprint arXiv:2109.07212* (2021). doi:10.48550/arXiv.2109.07212.
- [20] D-Wave hybrid solver service: An overview (14-1039A-B), accessed 2025-12-22 (Apr. 2022).

URL https://www.dwavesys.com/media/4bnpi53x/14-1039a-b_d-wave_hybrid_solver_service_an_overview.pdf

- [21] M. Koniorczyk, K. Krawiec, L. Botelho, N. Bešinović, K. Domino, Solving rescheduling problems in heterogeneous urban railway networks using hybrid quantum–classical approach, *Journal of Rail Transport Planning & Management* 34 (2025) 100521. doi:10.1016/j.jrtpm.2025.100521.
- [22] J. Pawłowski, J. Tuziemski, P. Tarasiuk, A. Przybysz, R. Adamski, K. Hendzel, Ł. Pawela, B. Gardas, Veloxq: A fast and efficient qubo solver (2025). arXiv:2501.19221.
URL <https://arxiv.org/abs/2501.19221>
- [23] J. Tuziemski, J. Pawłowski, P. Tarasiuk, Ł. Pawela, B. Gardas, Recent quantum runtime (dis)advantages (2025). arXiv:2510.06337.
URL <https://arxiv.org/abs/2510.06337>
- [24] P. Hanussek, J. Pawłowski, Z. Mzaouali, B. Gardas, Solving quantum-inspired dynamics on quantum and classical annealers (2025). arXiv:2509.03952.
URL <https://arxiv.org/abs/2509.03952>
- [25] R. Robertson, E. Doucet, Z. Mzaouali, K. Domino, B. Gardas, S. Deffner, Simon’s period finding on a quantum annealer (2025) 190–196doi:10.1109/qce65121.2025.00030.
URL <http://dx.doi.org/10.1109/QCE65121.2025.00030>
- [26] J. Pawłowski, P. Tarasiuk, J. Tuziemski, L. Pawela, B. Gardas, Closing the quantum-classical scaling gap in approximate optimization (2025). arXiv:2505.22514.
URL <https://arxiv.org/abs/2505.22514>
- [27] F. Glover, G. Kochenberger, Y. Du, A tutorial on formulating and using qubo models, arXiv preprint arXiv:1811.11538 (2018). doi:10.48550/arXiv.1811.11538.
- [28] B. Apolloni, C. Carvalho, D. De Falco, Quantum stochastic optimization, *Stochastic Processes and their Applications* 33 (2) (1989) 233–244. doi:10.1016/0304-4149(89)90040-9.
- [29] T. Kadowaki, H. Nishimori, Quantum annealing in the transverse Ising model, *Physical Review E* 58 (5) (1998) 5355. doi:10.1103/PhysRevE.58.5355.
- [30] E. Farhi, J. Goldstone, S. Gutmann, M. Sipser, Quantum computation by adiabatic evolution, arXiv preprint quant-ph/0001106 (2000). doi:10.48550/arXiv.quant-ph/0001106.

- [31] A. Lucas, Ising formulations of many NP problems, *Frontiers in Physics* 2 (2014) 5. doi:10.3389/fphy.2014.00005.
- [32] P. Date, R. Patton, C. Schuman, T. Potok, Efficiently embedding QUBO problems on adiabatic quantum computers, *Quantum Information Processing* 18 (2019) 1–31. doi:10.1007/s11128-019-2236-3.
- [33] T. Albash, D. A. Lidar, Adiabatic quantum computation, *Reviews of Modern Physics* 90 (1) (2018) 015002. doi:10.1103/RevModPhys.90.015002.
- [34] H. Oshiyama, M. Ohzeki, Benchmark of quantum-inspired heuristic solvers for quadratic unconstrained binary optimization, *Scientific reports* 12 (1) (2022) 1–10. doi:10.1038/s41598-022-06070-5.
- [35] S. Bolusani, M. Besançon, K. Bestuzheva, A. Chmiela, J. Dionísio, T. Donkiewicz, J. van Doornmalen, L. Eifler, M. Ghannam, A. Gleixner, C. Graczyk, K. Halbig, I. Hedtke, A. Hoen, C. Hojny, R. van der Hulst, D. Kamp, T. Koch, K. Kofler, J. Lentz, J. Manns, G. Mexi, E. Mühmer, M. E. Pfetsch, F. Schlösser, F. Serrano, Y. Shinano, M. Turner, S. Vigerske, D. Weninger, L. Xu, The SCIP Optimization Suite 9.0 (February 2024).
URL <https://optimization-online.org/2024/02/the-scip-optimization-suite-9-0/>
- [36] S. Bolusani, M. Besançon, K. Bestuzheva, A. Chmiela, J. Dionísio, T. Donkiewicz, J. van Doornmalen, L. Eifler, M. Ghannam, A. Gleixner, C. Graczyk, K. Halbig, I. Hedtke, A. Hoen, C. Hojny, R. van der Hulst, D. Kamp, T. Koch, K. Kofler, J. Lentz, J. Manns, G. Mexi, E. Mühmer, M. E. Pfetsch, F. Schlösser, F. Serrano, Y. Shinano, M. Turner, S. Vigerske, D. Weninger, L. Xu, The SCIP Optimization Suite 9.0 (24-02-29) (February 2024).
URL <https://nbn-resolving.org/urn:nbn:de:0297-zib-95528>
- [37] D-Wave Quantum Inc., Performance gains in the d-wave advantage2 system at the 4,400-qubit scale (14-1083A-A) (2025).
- [38] D-Wave Quantum Inc., D-wave announces general availability of advantage2 quantum computer (2025).
- [39] J. Janacek, M. Kohani, M. Koniorczyk, P. Marton, Optimization of periodic crew schedules with application of column generation method, *Transportation Research Part C: Emerging Technologies* 83 (2017) 165–178. doi:10.1016/j.trc.2017.07.008.